Planar Flow Field Measurements in Atmospheric and Pressurized Combustion Chambers

Chris Willert, Marc Jarius

Abstract The investigation of velocity fields in complex combustor flows is an important and necessary subject of propulsion technology. A persisting problem in CFD modeling is that current numerical design tools have a number of deficiencies in accurately predicting the complex combustor flow. Using planar techniques such as planar Doppler velocimetry (PDV) or particle image velocimetry (PIV) it is possible to provide detailed information of the flow field inside the combustor. This paper shall report on the status of applicability of PIV in combustor flows at realistic operating conditions.

1 Introduction

Given the current considerable growth of the air transport business, which is expected to last for the next few decades, the need arises to reduce both fuel consumption as well as the emissions of future aeroengines. Similar requirements apply to the power generation sector since the reliance on fossil fuels can not be replaced by regenerative energy sources in the near future. Current combustor design for both aeroengines and stationary power generators rely on extensive rig test programs, which are both expensive and time consuming, whereas the current numerical design tools have a number of deficiencies in accurately predicting the complex combustor flow and associated reactive chemistry. On this background the Institute of Propulsion Technology is involved in several national and European research programs that are aimed at providing industry with improved modeling tools for combustor design. A common strategy in these projects is to generate high quality CFD validation data from combustor configurations that share critical features of realistic combustors such as mixing jets, flame instabilities and increased operating pressures.

An important work package within these research programs is to provide detailed information of the flow field inside the combustor using single point measurement techniques such as laser Doppler anemometry (LDA) (Behrendt *et al.*, 1998, 2000; Hassa *et al.* 1999) and planar techniques such as planar Doppler velocimetry (PDV) (Röhle, 2000) or particle image velocimetry (PIV). PDV, also known in literature as Doppler global velocimetry (DGV), has been applied to isothermal test rigs (Röhle *et al.* 2000) and more recently to an atmospheric combustion chamber (Fischer *et al.*, 2000), and is a very promising technique for obtaining volumetric, time-averaged or phase-averaged flow fields. One of the primary advantages of PDV is that it is insensitive to optical distortions which are frequently encountered in fired combustion chambers (e.g. through changes in refractive index along the optical path). In principle, PDV should be applicable even in high pressure combustors where standard point measuring techniques (LDA) or point imaging techniques (PIV) falter due to increased beam steering effects, that is, the inability to focus the measurement volume, be it a LDA probe volume or discrete particles for PIV which become blurred. To date, many applications of PIV in flames reported in the literature have been restricted to small scale facilities or nearly laminar flow conditions (Han *et al.*, 2000; Stella *et al.*, 2000).

Disregarding the issues of seeding and illumination source for the moment, three component PDV measurements require either three observation directions, that is, three PDV camera systems, or three different light sheet propagation directions (or a combination of multiple cameras / multiple light sheets). For practical and economical reasons it is not always possible to provide the test rig with a sufficient number of access windows to meet this requirement. Several alternative approaches are under investigation to nevertheless enable three-component velocity measurements: (1) Multiple, flexible endoscopes could provide the camera with different viewing directions simultaneously thereby reducing the number of required light sheet directions. Another advantage of endoscopes is that they can view the flow through small access ports thus reducing the need for large viewing windows. (2) Another approach is to combine different planar velocity measurement

C. WILLERT, M. JARIUS
Institute of Propulsion Technology, German Aerospace Center (DLR), Köln, Germany

Correspondence to:
Dr. Chris WILLERT, Institut für Antriebstechnik, Deutsches Zentrum für Luft- und Raumfahrt (DLR),
D-51170 Köln, Germany, E-mail: chris.willert@dlr.de

techniques to provide three-component velocity data. In this case the combination of PIV with PDV is envisioned: Standard two-component PIV could be used to recover the in-plane velocity component, while PDV yields the out-of-plane velocity component. Compared to PDV, which was optimized at the institute for the measurement of time-averaged velocity data, PIV has the added advantage of providing instantaneous velocity maps. Of course, the calculation of velocity averages from PIV data requires significantly more processing and image data than PDV. This paper's intention is to report on the status of applicability of PIV in combustor flows with regard to a number of technological challenges that are not present in atmospheric/isothermal flows. Results of two recent PIV measurement campaigns on an atmospheric combustor and a pressurized combustor will be shown.

2
Experimental Facilities

The Institute of Propulsion Technology at the German Aerospace Center (DLR) has a wide variety of different sized combustor rigs for both industrial and research purposes at its disposal. Two experimental facilities were chosen for the PIV applicability study presented herein: (1) an atmospheric 'laboratory-scale' combustor with a double swirl nozzle and either gas or kerosene fueling, (2) a pressurized, single sector combustor (SSC, e.g. one fuel nozzle) with optical access from three sides (Behrendt *et al*., 1998). The former facility is rather simple in its maintenance/operation and lends itself to the optimization of laser-optical measurement equipment. As shown in Figure 1 one wall is fitted with a glass window for optical access of the CCD camera. To permit light sheet passage through the center plane the combustion chamber is fitted with a pair of narrow rectangular flanges which are sealed off by narrow glass windows. The windows and the flanges are flushed with cold air to protect them from particles and thermal strain. Although the presence of these flanges is not typical of realistic combustors they greatly reduce laser light scatter within the field of view and thus improve signal quality of PIV and PDV.

The pressurized single sector combustor (SSC), schematically shown in Figure 2, can be operated at up to 20 bar with air pre-heating of up to 850 K at mass flow rates of 1.3 kg/s. The nozzle plenum is supplied with pre-heated primary air downstream of a critical throttle. The primary air is split in a 2:1 ratio and guided into the double swirl nozzle and the inner window cooling slits, respectively. To reduce the area of (axial) recirculation above the nozzle pre-heated secondary air is introduced at the half length of the combustion chamber. Figure 3 shows a photograph of the pressurized SSC in operation. Operational costs in terms of manpower and primary energy are not insignificant, such that tests must be well prepared in advance.

Both test rigs have similar internal combustor dimensions, that is, a square cross section with a side length of about 100 mm and a double swirl blast atomizer nozzle centered in the bottom plate. Kerosene fueling was used in the measurements presented herein.

For the PIV measurements the laser light sheet was placed through the center of the chamber as shown in Figures 1 and 2 with the recording CCD camera placed normal to this plane. Illumination was provided by a standard, frequency-doubled, double-cavity Nd:YAG laser (NewWave, Gemini PIV) with a pulse energy of up to 120 mJ per pulse at 532 nm. On the recording side, a thermo-electrically cooled, interline transfer CCD camera (PCO, 1280 x 1024 pixel resolution) with a f = 55 mm, f # 2.8 lens (Nikon) was used. A bandpass filter with center frequency 532 nm and width 5 nm (FWHM) placed in front of the lens rejected most of the unwanted radiation. The pulse delay between the laser pulses varied between $\tau = 3$ µs and $\tau = 4$ µs.

For the measurements in the atmospheric chamber solid tracer particles (SiO_2, 0.8 µm, Merck) were introduced into the cold air flow upstream of the air blast nozzle using a simple, fluidized-bed particle dispenser. In the SSC a more complex fluidized bed particle dispenser (Figure 4, left), designed for pressures exceeding 40 bar, introduced seeding (SiO_2, 2 µm, Merck) into the preheated air stream upstream of the fuel nozzle. At its exit, this dispenser has a sonic flow orifice with high flow gradients that are intended to break up any larger agglomerations of the seeding material.

3
Examples of Results

In the following, some exemplary experimental results are presented. With regard to PIV processing standard correlation algorithms were used with an interrogation window size of 32 x 32 pixel and a 50 % overlap. For clarity, only every other row of PIV vectors are shown in the plots.

The measured flow field from the atmospheric burner are shown in Figure 5. On the left side the mean value of the velocity distribution, calculated from 100 PIV images, is presented as a vector plot (right) and, for clarity, also as a contour plot of the velocity magnitude (left). In this context it should be mentioned that in areas of high

kerosene droplet content (eg. in the lobes of the spray cone), the velocity measurement is a combination of gas- and fuel droplet velocity. Although the two velocities are difficult to seperate in the PIV data, recent PDV applications on the same combustor demonstrated that the slip velocity can be estimated (Fischer *et al.*, 2000). The results shown in Figure 5 are quite typical for this rather simple burner with the exception that only a very small axial recirculation area is present above the middle of the nozzle (x = 0 mm, y = 10 mm). The flame is mainly stabilized by corner vortices. The remaining recirculation area is not entirely symmetric, which is mainly an artifact of not having the light sheet accurately centered above the nozzle. The influence of the swirl dominate the orientation of the recirculation. The opening angle of the flame is about 30°. Higher velocities exist only directly at the exit of the nozzle. Since this atmospheric burner was operated without a pre-heating of the air the flame burns a short distance over the exit of the nozzle. The air fuel ratio is in the range of 13.

Roughly 15 mm above the nozzle the flow field around the spray cone exhibits a small indentation. An interpretation of that phenomenon is that the atomization process in the swirl nozzle generates small droplets as well as large ones. Since the larger droplets do not follow the flow they tend to fly out of the strongly swirling flow field into almost stationary air. Meanwhile the kerosene droplets continue to evaporate and partially are sucked back into the main combusting flow. Larger droplets tend to fly past the main combustion zone, and evaporate slower. Images of these larger droplets and their high relative velocity are shown in Figure 9. In this regard it should be recalled that this atmospheric burner was mainly designed for measurement equipment tests; it represent not a modern burner for aeroengines or stationary power generators. A better comparison could be achieved if air pre-heating is utilized.

In Figure 6 the measured flow field from the single sector combustor is presented, with the mean velocity vector map shown on the left and a corresponding velocity magnitude contour plot shown on the right. The combustor was operated at 3 bar of pressure with an air pre-heating temperature of 700 K and air-to-fuel ratio of 30. During the experiment only 13 well-seeded PIV image pairs could be obtained which was due to the intermittent operation of the seeding generator. Nevertheless, the obtained velocity data are more typical of realistic burner configurations. The flow exhibits a relatively large recirculation area centered above the nozzle. Compared to 60 m/s exit nozzle exit velocity, the downward velocity in the recirculation flow exceeds velocities up 20 m/s close to the nozzle which results in high, turbulence generating, shear rates in this area. The recirculation also carries unburned radicals of the hot fuel-air mixture back toward the nozzle which has a stabilizing effect on the flame's position and ensures a continuous and complete combustion. Together with the corner vortices outside and below the spray cone the combustion in the SSC is very stable. Compared to the atmospheric combustor the opening angle of the shear layer (e.g. high velocity region) at about 60° is significantly larger, although the spray cone has a similar opening angle. The recorded images also showed the presence of larger droplets far downstream of the nozzle with convective velocities strongly differing from the surrounding flow.

A comparison of instantaneous velocity maps of the flow inside the atmospheric and the single sector combustor are shown in Figures 7 and 8. Visually the flow inside the atmospheric combustor is less structured than in the SSC. Turbulent flow is distributed in across the entire flame area as can be seen in the accompanying vorticity map (Figure 7, right). On the other hand, the instantaneous velocity and vorticity maps of the SSC show closer resemblance to the averaged result shown in Figure 6. The described recirculation area is easy to identify and is characterized by the lack of vortical flow between the lobes of the spray cone. The flow in the spray cone area resembles that of a turbulent shear layer, that is, periodically spaced vortical structures can be identified. By contrast the atmospheric combustor shows neither the quiescent recirculation region nor clearly identifiable shear layers. In this case the flow immediately above the nozzle exhibits strong shear and some reverse flow. Further downstream the flow broadens and shows a wide spatial distribution of turbulent structures. The presence reduced recirculation is generally an indication of a small swirl (circumferential velocity around the nozzle axis) (Beér *et al*. 1972).

Although both combustors are equipped with similar nozzles (in terms of observed spray cone angle) the differences in the flow can be attributed, to a large extent, to the lack of preheating in the atmospheric combustor. While the combustion is present immediately above the nozzle in the SSC, the atmospheric combustor exhibits combustion only on the outside of the spray cone. This can also be seen in OH-LIF data of the atmospheric combustor (Fischer *et al*. 2000).

4
Observations, Encountered Problems and Solution Strategies

In the course of the measurements several issues characteristic of applying PIV in liquid fuel fired combustion chambers could identified and are described in the following.

Mie scattering off fuel droplets: The atomizer's primary function is the dispersion of the liquid fuel into small droplets that can rapidly evaporate in the combustion zone downstream. Larger droplets can survive far downstream as illustrated in Figure 9a which shows a portion about 30 mm downstream of the nozzle. As can be seen in Figure 9d, the PIV analysis of such images locks into the droplet velocity and hides the underlying gas velocity. The actual seeding particle images are much weaker – in this case about 5-10% compared to that of the fuel droplets. In order to better estimate the gas velocity the images were first preconditioned using a high-pass filter and local intensity equalization (Figure 9c) as suggested by Willert (1997). This matched seeding particle image intensity to that of the fuel droplets and since the seeding particle number density generally is higher, the PIV analysis locks into the displacement of the seeding and thereby estimates the gas velocity (Figure 9e). However, this approach only works in cases where the number density of droplets is low in comparison to the seeding particles. Immediately downstream of the nozzle the fuel droplets outnumber the particle images and bias the measured velocity to that of the droplets. As a result a combination of gas and droplet velocity is measured. In principle the mean velocity of the kerosene droplets could be measured by recording images without particle seeding. This has been demonstrated by Fischer *et al.* (2000) using PDV.

Flame luminosity: Stoichiometrically balanced or fuel-lean, atmospheric flames generally exhibit little flame luminosity, a fuel-rich flame under increased pressure, on the other hand, is very bright, mainly due to soot glowing (the seeding glows as well!). This flame luminosity can be reduced by placing a narrow-bandwidth laser interference filter in front of the sensor or collecting lens. However, the time-delayed read-out of the second PIV image ó an artifact of the double-shuttered, interline transfer CCDs (Figure 10) ó in conjunction with the residual light transmittance of the filter, results in the accumulation of the flame luminosity on the sensor (typically > 100 ms). Under certain test facility operating conditions, this additional light exceeded the dynamic range of the sensor, making a successful PIV measurement impossible. One possible solution to this problem is to place a fast response liquid crystal polymer (LCP) scattering shutter in front of the sensor. These shutters are based on electrically controllable light scattering and, opposed to conventional LCDs, require no polarizers making them highly transparent. In the 'closed' state otherwise freely moving liquid crystals group into clusters that scatter incoming light causing the system to turn highly turbid. As a consequence of this operating principle, the shutter can only destroy image contrast. A DC light intensity level is still transmitted. Placed in front of a lens, the model shown in Figure 11 (Philips Optics) has a open-closed response time of 1 ms and an extinction better than 95% which is sufficient for most of our combustion applications.

Window contamination by seeding: A common problem encountered in seeding flows with solid particles is the tendency of seed material depositing onto access windows thereby rendering them optically opaque. The high pressure test rig uses forced air cooling on the inner liner windows such that this effect was reduced. Over time, seeding did accumulate on the four side walls of the chamber. This resulted in scattering of the main laser light sheet as it passed the inner liner windows of the SSC. As a result of this the entire volume was diffusely illuminated (up to 25% of the camera's dynamic range). Seeding residue deposited on the viewing window was equally illuminated such that a stationary 'particle' image pattern was produced. In some circumstances this resulted in a zero-velocity measurement. Due to lens defocusing at lower f-numbers this effect could be reduced. PIV measurements close to either of the viewing windows would not have been possible. Since the seeding contamination itself is difficult to tackle another approach is to reduce the possibility of laser light scatter by recessing the access windows from the chamber side walls. This was realized in the atmospheric combustor and is shown in Figure 1 and is a method of choice in upcoming future applications of PIV and PDV.

Seeding: The most challenging aspect in seeding flows with typically non-spherical, solid particles is to maintain a controlled and steady production rate. The fluidized-bed, seeding generator (Figure 4) with its de-agglomeration sonic orifice did not perform entirely satisfactory for several reasons. The initially homogeneous powder in the bed has a tendency to agglomerate into larger clumps such that a steadily decreasing amount of seeding material is carried to the exit orifice. Due to the relatively small surface size of the sintered metal filter not all particles are mixed in that process. On the other hand, the larger particles passing through the sonic orifice act abrasively on the slit – the seeding particle diameter can not be maintained (clogging of the orifice and even the ducts downstream is also possible). Several improvements of the seeding device are currently under way: 1) A stirring device inside the fluidized bed is intended to prevent the formation of larger clumps. By also

forcing air out of the stirrer's blades it is possible to further agitate the seeding bed. In a next step three curved metal wings will be mounted on the end of the stirring device with the intention of grinding the larger agglomerates. 2) The sintered metal filter cone is replaced by a sintered glass filter plate (Borosilicate glass 3.3; ROBU®). The glass filters are divided into seven porosity classes from 1.0 µm ó 500 µm. The choice of porosity depends on the seeding diameter. In this case the glass filter with a porosity in a range of 100...160 µm is used.

Alternative approaches such as the dispersion of liquid suspensions of solid particles as suggested by Wernet *et al.* (1995) are also under investigation. However, depending on the amount of liquid particle suspensions added to the preheated air stream the method of seeding is likely to have an effect on the flame (cooling by evaporation, changed reactive chemistry).

5
Conclusions

The presented experiments were mainly intended to assess the feasibility of applying PIV in combustors used for applied combustion research. The results have shown that it is possible to apply PIV in an atmospheric combustor as well as a pressurized combustor at 3 bar. At 6 bar particle images could still be identified but the intermittent operation of the seeding generator did not permit the acquisition of good quality PIV recordings. Experiences gained in the past application of a variety of other measurement techniques have shown that techniques relying on imaging single points within the flow (e.g. LDA, CARS) begin the falter at higher pressures (12 bar at 300 mm optical penetration depth, Hassa *et al.* 1999). PIV is expected to have similar restrictions. The defocusing of a point within the (hot) flow is a result of refractive index gradients along the optical path which are caused through the combination of temperature gradients, density variations and varying gas composition.

Aside from the operational pressure, the optical penetration depth is a critical factor that dictates the degree of defocusing. The data given herein were obtained in a plane approximately 50 mm from the front window. Larger facilities would require penetration depths of up to 300 mm. To some extent the defocusing can be controlled by reducing the recording lens aperture, that is, by reducing the opening angle of the optical cone, because this limits the amount of index gradients across the optical path. LDA is very susceptible to this effect since it relies on crossing two laser beams from two different directions, typically at about 10° opening angle. For the PIV measurements f # 8 was used which corresponds to an opening angle of less than 0.3°. This gives rise to our speculation that PIV measurements should be possible in cases were single point measurement techniques like LDA begin to fail. However, given the successful imaging of discrete particles does not guarantee that the degree of beam steering varies between the exposures of the PIV recording. It is therefore possible that the apparent (measured) position of a particle image differs from its true position and therefore may influence the displacement measurement. The amount of actual beam steering between the two PIV exposures has been investigated by Han *et al.* (2000) for a laboratory-scale hydrogen flame and was found to be within 0.1 pixel. For the data presented here this would correspond to a measurement uncertainty on the order of 1 m/s. However, reliable estimates for larger flames are currently not available. A possible approach to estimate the amount of beam steering is to measure the integral displacement using the background oriented schlieren (BOS) method proposed by Richard *et al.*, 2000.

In cases were PIV even becomes unsuccessful planar Doppler velocimetry may be a viable alternative since it does not rely on imaging discrete particles and rather collects the integral light scattered many particles. However current implementations of PDV cannot reliably measure the unsteady flow and therefore are restricted to the measurement of mean values. Overall the potential of PIV in combustion research could be demonstrated herein and encourage further investigations. Once remaining problems such as seeding can be resolved both PIV and PDV show great promise.

References

Beér, J.M., Chigier N.A., (1972) "Combustion Aerodynamics", Applied Sciences Publishers, London.

Behrendt T., Frodermann M., Hassa C., Heinze J., Lehmann B., Stursberg K. (1998), "Optical measurements of spray combustion in a single sector combustor from a practical fuel injector at higher pressures", RTO AVT Symposium on Gas Turbine Engine Combustion, Emissions and Alternative Fuels", Lisbon, Pt.

Behrendt T., Carl M., Fleing C., Frodermann M., Heinze J., Hassa C., Meier U., Wolff-Gaßmann D., Hohmann S., Zarzalis N. (2000), "Experimental and numerical investigation of a planar combustor sector at realistic operating conditions", ASME TURBO EXPO 2000, Munich, Germany, Paper 2000-GT-0123.

Fischer M., Heinze J., Matthias K., Röhle I. (2000), "Doppler Global velocimetry in flames using a newly developed, frequency stabilized, tunable, long pulse Nd:YAG laser", 10th Symposium of Applications Laser Techniques to Fluid Mechanics, Lisbon, Pt.

Han D., Su L.K., Menon R.K., Mungal M.G. (2000), "Study of a lifted-jet flame using a stereoscopic PIV system", 10th Symposium of Applications Laser Techniques to Fluid Mechanics, Lisbon, Pt.

Hassa C., Carl M., Frodermann M., Behrendt T., Heinze J., Röhle I., Brehm N., Schilling T., Doerr, T. (1999), "Experimental investigation of an axially staged combustor sector with optical diagnostics at realistic operating conditions", RTO-MP-14, pp. 18-1 – 18-11.

Stella A., Guj G., Kompenhans J., Raffel M., Richard H. (2000), "Application of particle image velocimetry to combusting flows: design considerations and uncertainty assessment", Exp. Fluids, 30, (No. 2), pp. 167-180 Experiments in Fluids

Richard H, Raffel M., Rein M., Kompenhans J. (2000), "Demonstration of the applicability of a background oriented schlieren (BOS) method", 10th Symposium of Applications Laser Techniques to Fluid Mechanics, Lisbon, Pt.

Röhle I. (2000), "Doppler global velocimetry", in RTO Lecture Series 217, Planar Optical Measurement Methods for Gas Turbine Components, Neuilly-Sur-Seine Cedex, France.

Röhle I., Schodl R., Voigt P., Willert C. (2000), "Recent developments and applications of quantitative laser light sheet measuring techniques in turbomachinery components", Measurement Science and Technology, Vol. 11, pp. 1023-1035.

Wernet M.P., Skoch G.J., Wernet J.H. (1995), "Demonstration of a stabilized alumina/ethanol colloidal dispersion technique for seeding high temperature air flows," Intl. Congress on Instrumentation in Aerospace Simulation Facilities (ICIASF), Ohio, U.S.A.

Willert C. (1997), "Stereoscopic digital particle image velocimetry for application in wind tunnel flows", Measurement Science and Technology, Vol. 8, pp. 1465-1479.

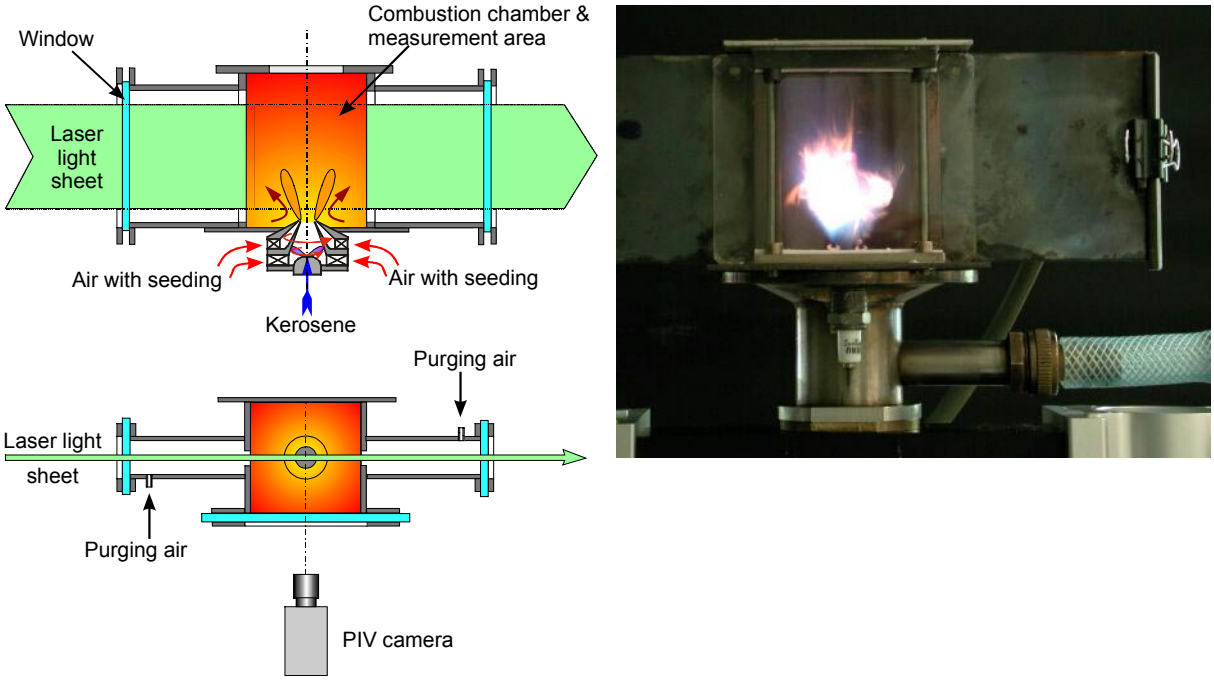

Fig. 1. Schematic (front and top view) and photograph of the atmospheric combustion chamber.

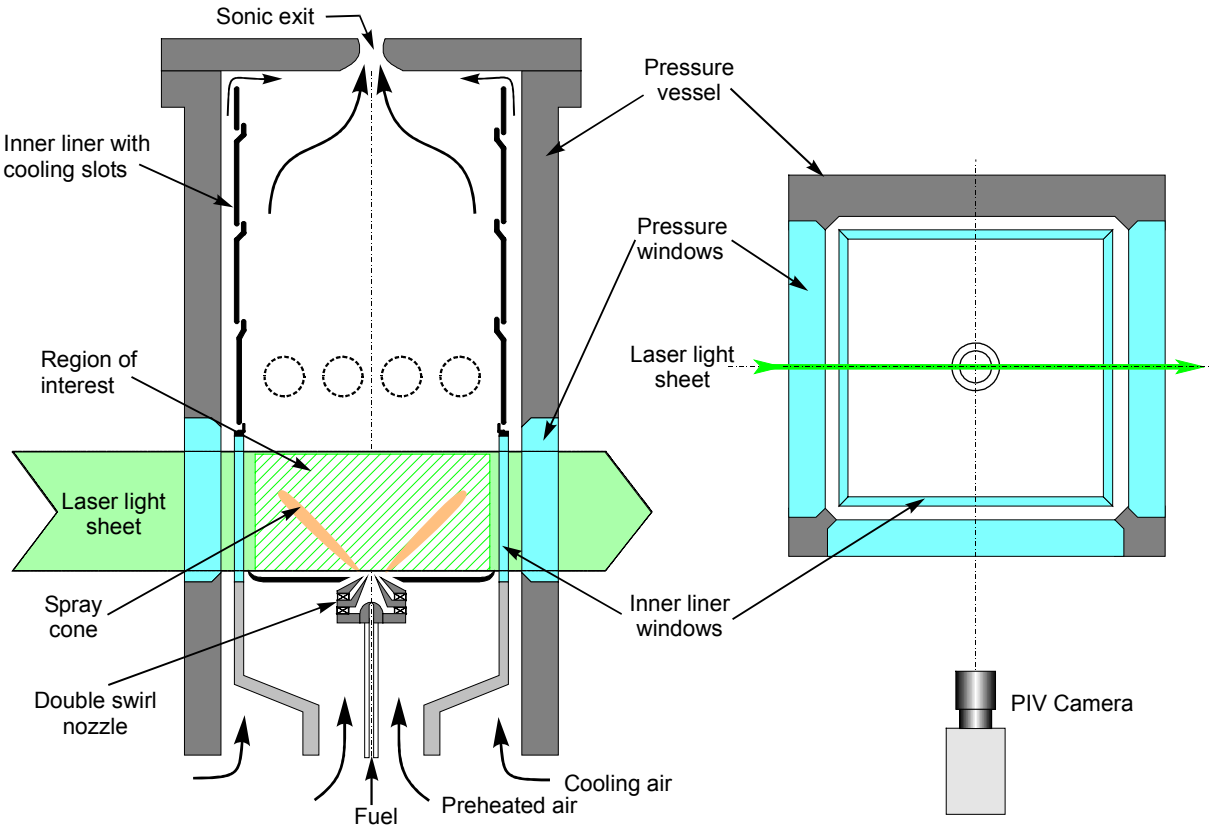

Fig. 2. Schematic of the single sector (front and top view), high pressure combustion chamber.

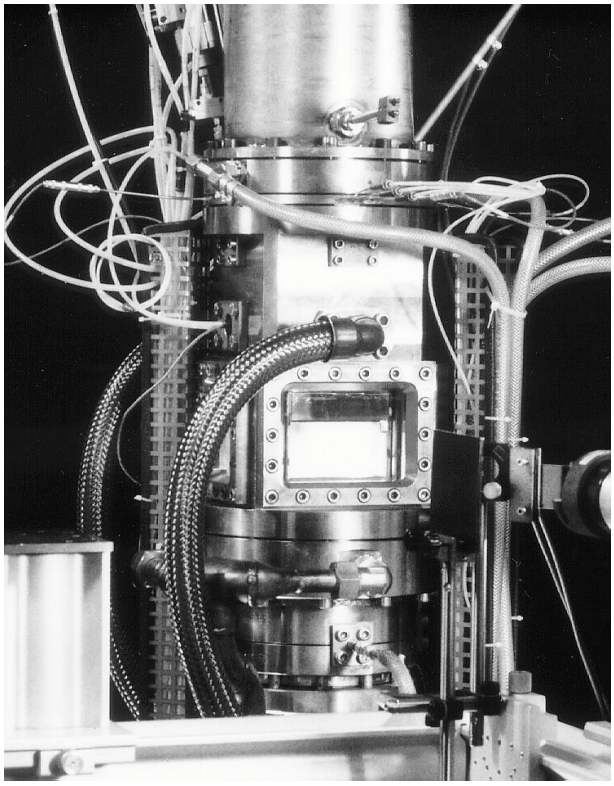

Fig. 3. Photograph of the pressurized, single sector combustor

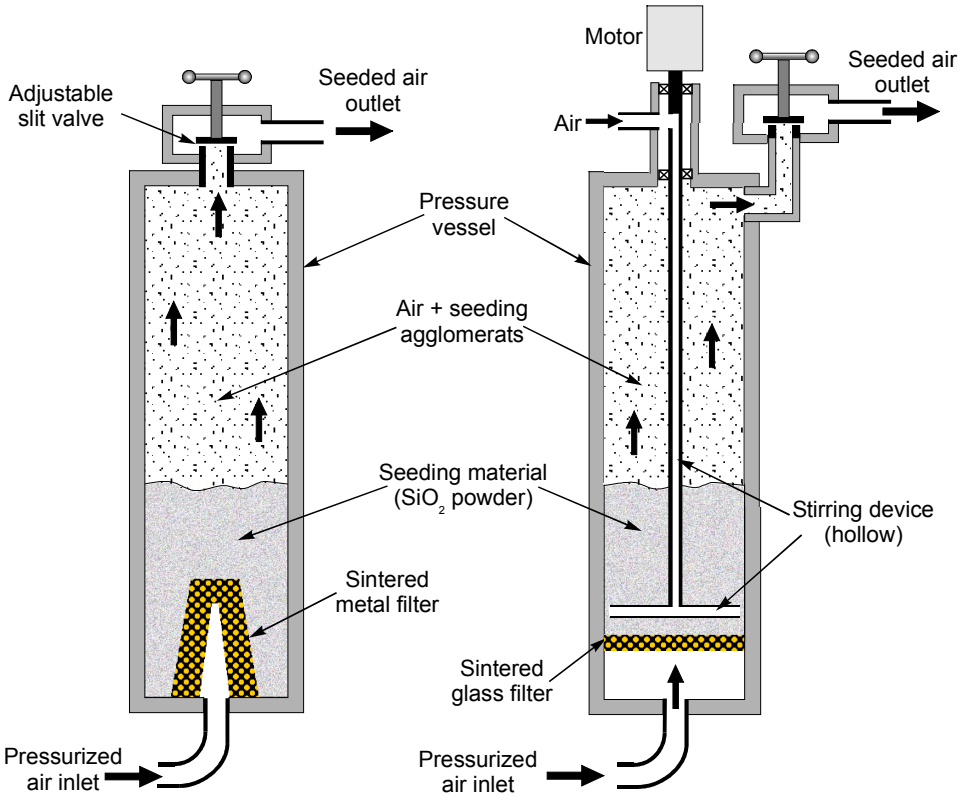

Fig. 4. Fluidized bed seeding generator for operation up to 40 bar, simple version (left) and modified with stirring device (right)

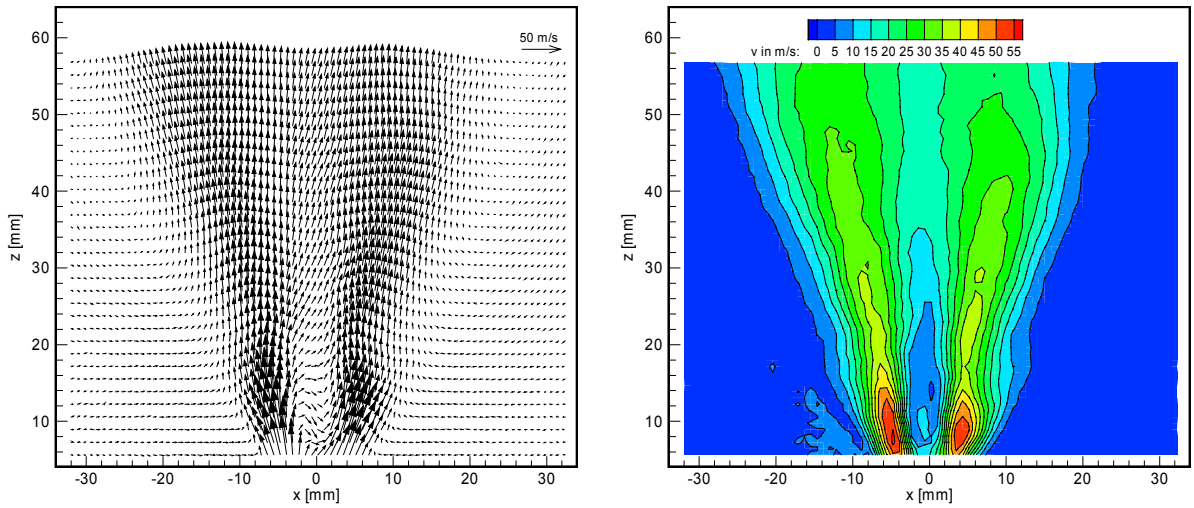

Fig. 5. Average of 100 PIV images of the flow inside the atmospheric combustor.

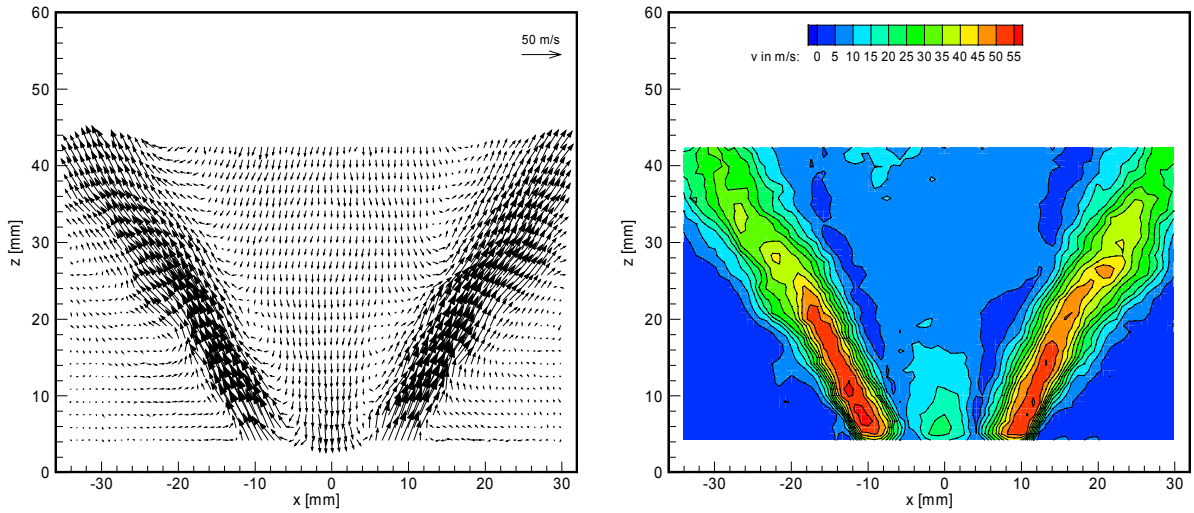

Fig. 6. Average of 13 PIV images of the flow inside the pressurized single sector combustor at 3 bar.

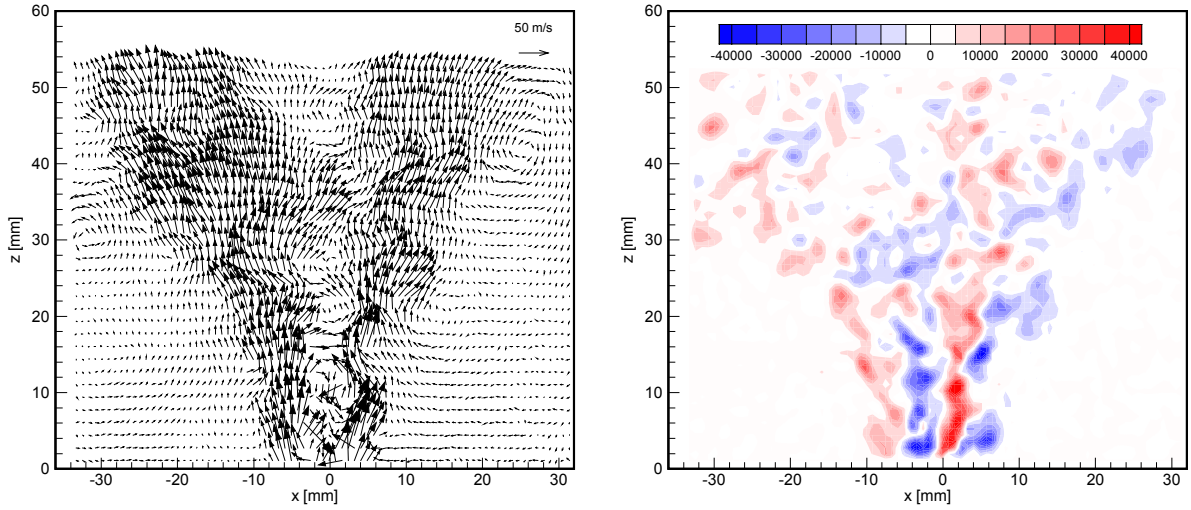

Fig. 7. Example of instantaneous flow inside the atmospheric combustor: velocity vector map (left), and vorticity map (right). (The vorticity component normal to the plane, ω_y , is shown).

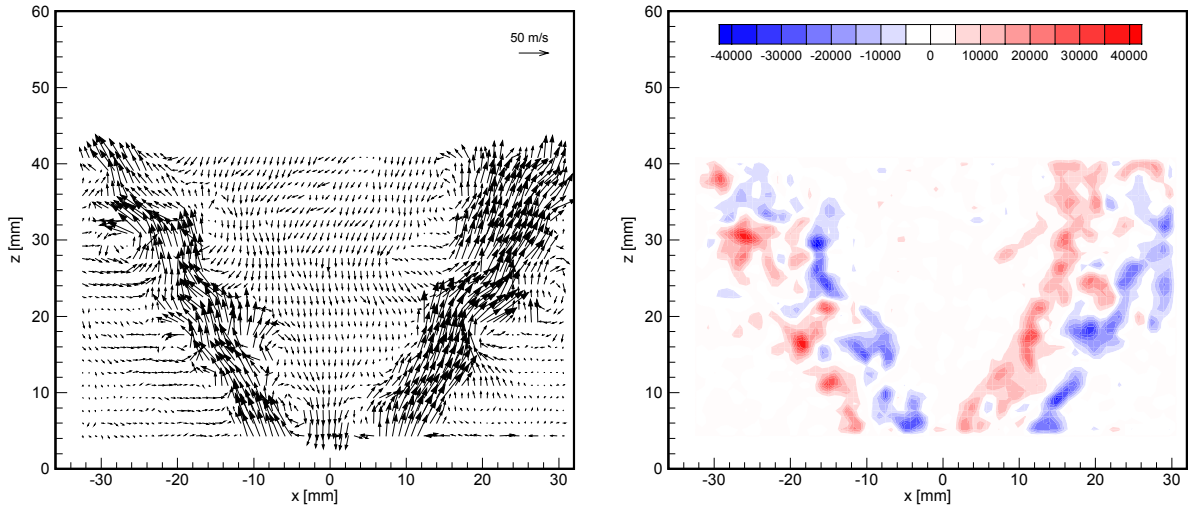

Fig. 8. Example of instantaneous flow inside the pressurized single sector combustor operating at 3 bar: velocity vector map (left), and vorticity map (right). (The vorticity component normal to the plane, ω_y , is shown).

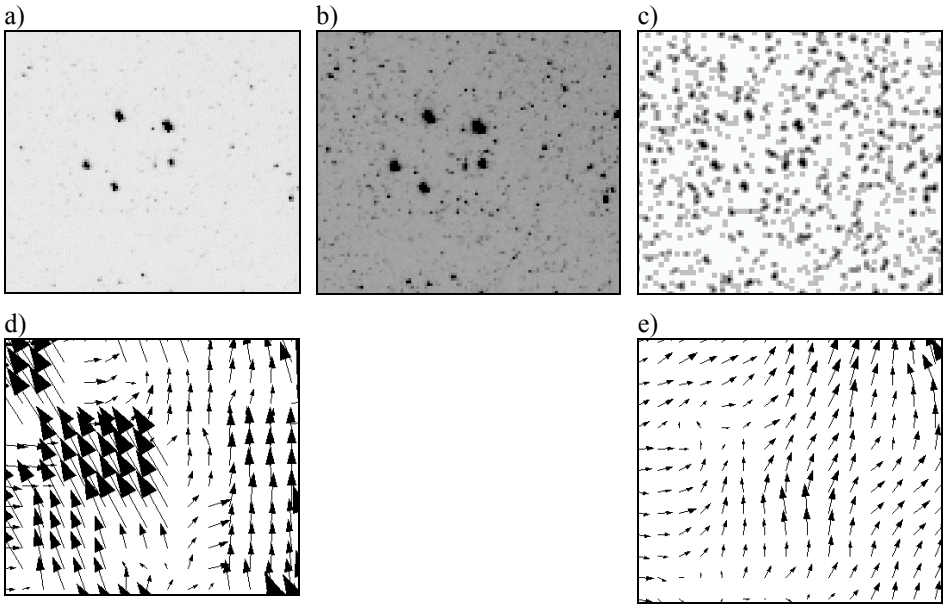

Fig. 9. Portion of PIV recordings - inverted for clarity - and processed PIV data: a) fuel droplets, b) brightened version of a) with seeding visible, c) pre-processed image, d) flow field after standard PIV analysis, e) flow field obtained after enhancement of PIV images. (The shown image portion is about 110 pixels wide.)

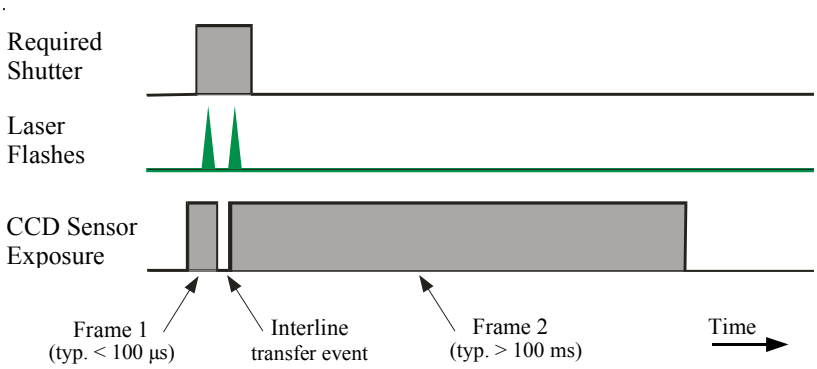

Fig. 10. PIV-Camera timing sequence illustrating increased light sensitivity of frame 2.

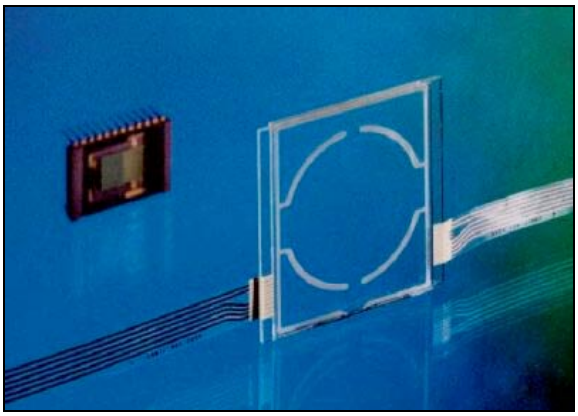

Fig. 11. Liquid crystal polymer (LCP) scattering shutter